Ab Initio Investigation of Gadolinium Complexes with Polyamino Carboxylate Ligands and Force Fields Parametrization of Metal−Ligand Interactions

Ugo Cosentino,* Giorgio Moro, Demetrio Pitea, and Alessandra Villa

Dipartimento di Chimica Fisica ed Elettrochimica, Università degli Studi di Milano, via Golgi 19, 20133 Milano, Italy

Pier Carlo Fantucci

Dipartimento di Chimica Inorganica, Metallorganica e Analitica, Università degli Studi di Milano, via Venezian 21, 20133 Milano, Italy

Alessandro Maiocchi and Fulvio Uggeri

Bracco SpA, Via E. Folli 50, 20134 Milano, Italy

Received: October 8, 1997; In Final Form: March 4, 1998

The conformational properties of five gadolinium(III) complexes with polyamino carboxylate (PAC) ligands used as magnetic resonance imaging contrast agents have been investigated by ab initio and molecular mechanics (MM) methods. Ab initio calculations were performed using an effective core potential (ECP) that includes 4f electrons in the core and an optimized valence basis set for the metal. To test the reliability of ECP calculations, full geometry optimizations of Gd complexes were performed at the RHF and DFT (B-LYP) levels using the 3-21G and the 6-31G* basis sets for the ligands. Comparison with experimental data shows that ab initio calculations provide quite accurate geometries and correct conformational energies at the RHF level. Within the framework of a valence force fields, parameters for Gd−ligand interactions were determined by fitting the empirical potential to the ab initio potential energy surface (PES) of the [Gd−DOTA(H_2O)]$^{-1}$ complex. Sampling of the PES was performed by moving the ion into the frozen coordination cage of the ab initio optimized geometry; for each generated structure the energy and first derivatives, with respect to the Cartesian coordinates of the metal and donor atoms, were calculated at the RHF level using both 3-21G and 6-31G* basis sets for the ligand. For each considered basis set, two sets of parameters, with the electrostatic contribution turned on or off in the force fields, were determined. All the implemented sets of parameters provide reliable molecular geometries for PAC complexes, but only sets derived including the electrostatic contribution correctly reproduce the observed trend of conformational energies.

I. Introduction

In the last two decades magnetic resonance imaging (MRI) has become an important diagnostic tool in modern medical imaging.[1,2] MRI is a technique based upon a spatially localized NMR signal of the ^{1}H nucleus of in vivo water molecules. To increase signal intensity and enhance contrast in the MR images of diseased and normal tissues, a paramagnetic substance, able to catalyze the relaxation rates of water protons via dipolar interactions, is administered to the patient. Lanthanide complexes with polyamino carboxylate (PAC) ligands, particularly those of the highly paramagnetic Gd(III) ion, are the most widely employed contrast agents for MRI.[3]

A rational design of new MRI contrast agents requires the detailed understanding of the structure and dynamics of Gd−PAC complexes to assess those factors that can lead to compounds with desired properties.[4,5] Experimental investigations on the behavior of Gd complexes in solution cannot be easily performed, as the usual techniques, such as NMR spectroscopy, are not suitable due to the high magnetic moment of the Gd ion. Thus, a theoretical investigation of Gd complexes effectively represents a valid tool for the characterization of their molecular properties. In this paper, the setting up of reliable computational methods for modeling Gd complexes is presented. Five complexes of Gd with macrocyclic (DOTA, DOTMA, DO3A, and DO3MA) and linear (DTPA) PAC ligands[6] are investigated (Figure 1); currently, compounds **1** and **5** are the most widely used contrast agents in clinical practice.

With respect to "usual" organic molecules, ab initio calculations on Gd complexes present additional problems due to the presence of the metal. In fact, the Gd ion involves a great number of electrons, an incompletely filled 4f shell, and large relativistic and correlation effects. Restriction of the quantomechanical treatment to the valence shell of the lanthanides by means of effective core potential (ECP) provides an efficient way to reduce the computational effort and to incorporate relativistic effects into self-consistent-field (SCF) calculations.[7,8] ECPs differing in core size have been developed for lanthanides[9−12] and tested on simple lanthanide systems: hydrides, oxides, and halides.[13−18] In the present work, the ECP considering (1s−4d, 4f ^{n}) core electrons is used:[12] inclusion of 4f electrons into the core makes this ECP more suitable to deal with molecular systems of large dimensions, as shown in the case of lanthanide(II) metallocenes[19] and the Gd(III) nonaaquo ion.[20]

* To whom correspondence should be addressed. Phone: ++39 2 26603254. Fax: ++39 2 70638129. E-mail: ugo@sg2.csrsrc.mi.cnr.it.

S1089-5639(97)03271-4 CCC: $15.00
Published on Web 05/22/1998

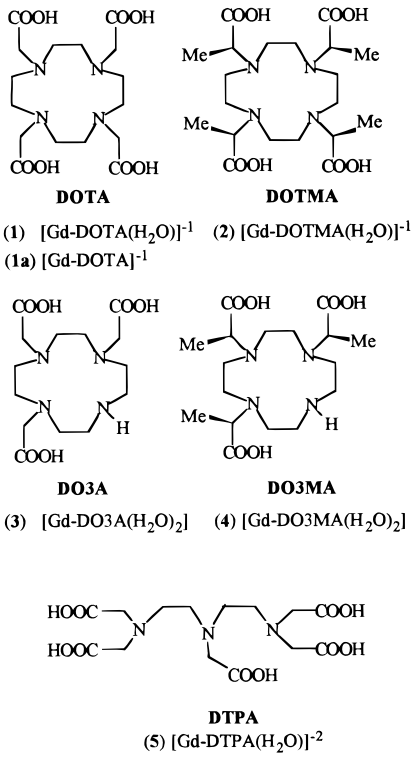

Figure 1. Sketches of the considered PAC ligands and numbering of the investigated Gadolinium complexes.

However, due to the molecular dimensions of the considered Gd−PAC complexes, ab initio methods are not suitable for systematic investigations even with the ECP approximation. A reliable alternative for the study of complex systems is the molecular mechanics (MM) method. The continuing efforts in developing potential functions, and related parameters suitable for the description of the metal−ligand interactions, make MM increasingly important in the area of coordination chemistry.[21−23] In the case of lanthanides, force fields derived from experimental data are available.[24−27] However, because experimental data on Gd complexes are available only for a few classes of ligands, a more general strategy for the parametrization of Gd−ligand interactions would be preferable. Indeed, parametrization can be performed by fitting the MM empirical potential to the potential energy surface (PES) calculated by ab initio methods; in this case the quality of the force fields depends on PES quality, but is not limited by the lack of lab experiments. Recently, a methodology based on the fitting of the empirical potential to the ab initio PES described by the energy and the energy derivatives was developed[28] and applied to develop de novo force fields for several molecular systems.[29−31] In this paper, the parametrization of the Gd−PAC ligand interactions performed by means of this methodology is reported. The procedure is aimed at determining, from the ab initio PES, only the parameters concerning the metal−ligand interactions, the intraligand interactions being described by means of a predefined force fields; therefore, the parameters are determined by reproducing the ab initio potential around the ion and not the whole PES of the complex. As the accuracy of the ab initio PES is crucial to obtaining reliable force fields, considerable effort has been spent in this work to investigate the reliability of ab initio methods using ECP.

The organization of this paper is as follows: section II describes the computational methods employed in quantomechanical calculations and the results on the considered Gd−PAC complexes; section III presents the force fields parametrization procedure and the obtained parameters; section IV discusses results of MM calculations.

II. Ab Initio Calculations on Gd−PAC Complexes

Methods and Results. Calculations on Gd−PAC complexes were performed with the Gaussian94 program[32] using the (1s−4d, 4f [7]) ECP with the [5s4p3d]-GTO valence basis set for the metal[12] and the 3-21G and 6-31G* basis sets for the PAC ligands.

Full geometry optimizations of compounds **1**−**5** were performed at the RHF level;[33] the calculated stationary points were not characterized because analytical second derivatives are not implemented in Gaussian94 for ECP, and numerical differentiation is a very time-consuming procedure that exceeds the available computational resources.

To test the effects of electron correlation, the octa-coordinated $[Gd-DOTA]^{-1}$ complex **1a** (Figure 1), which presents C_4 symmetry, was optimized at the DFT level, using the B-LYP[34] functional, with the 6-31G* basis set. Moreover, B-LYP/6-31G* energy calculations were performed on the optimized RHF geometries of compound **1**.

According to the experimental evidence (see Discussion), calculations were performed on two isomers of compounds **1**−**4** and on one isomer of compound **5**. When available, the crystallographic structures were used as starting geometries.

Experimental and calculated values for the main geometrical parameters of compounds **1**−**5** are reported in Table 1; the calculated conformational energies of compounds **1**−**4** are reported in Table 2.

Discussion. For each of compounds **1**−**4**, calculations provide two minimum energy conformations. In both conformational isomers (Figure 2) the ion is ennea-coordinated and the coordination polyhedron is a distorted square antiprism, capped by one water molecule. The acetate arms are oriented around the Gadolinium ion in a propeller-like manner, assuming a clockwise (Δ) or a counterclockwise (Λ) orientation; the tetraaza macrocyclic ring adopts a [3333] square conformation[35] with ($\lambda\lambda\lambda\lambda$) helicity.[36] In the two isomers the parallel squares, defined by the nitrogen and the oxygen atoms, respectively, are staggered by a ϕ angle (Figure 3) with opposite sign: thus, the $\Delta(\lambda\lambda\lambda\lambda)$ isomer is labeled as antiprismatic (**A**) and the $\Lambda(\lambda\lambda\lambda\lambda)$ as inverted antiprismatic (**IA**).

Experimental evidence, both in the solid state[37,38] and in solution,[39−42] show that DOTA and DOTA-like complexes can effectively present two conformational isomers. The calculated **A** and **IA** conformations indeed correspond to the crystallographic structures observed in compounds **1**,[43] **3**,[44] and **4**.[37]

According to the crystallographic structure[45] and to the experimental evidence in solution,[46] in the calculated structure of compound **5** the ion is ennea-coordinated with a distorted tricapped trigonal prism coordination geometry (Figure 4).

Geometries. The overall agreement between the experimental and the calculated structures is highlighted by the average values of the root-mean-square (rms) calculated on the Cartesian coordinates (Table 3) and by the superimposition of experimental and ab initio structures (Figure 5). The agreement is still satisfactory (Table 3) when rms values are evaluated (compounds **3**−**5**) by matching the calculated water positions with the corresponding positions that are occupied by carboxylic oxygens in the experimental structure. In fact, in these compounds, which present dimeric or trimeric structures in the solid state, no water molecules are coordinated to the ion because the corresponding coordination positions are occupied by

TABLE 1: Values of the Main Geometrical Parameters of Experimental and ab Initio Calculated Structures of Compounds 1−5 (See Figures 3 and 4 for Atomic Numbering). The Average Values Are Reported with Standard Deviations in Parentheses. Distances (Å), Angles (deg)

	Exp.	RHF/3-21G	RHF/6-31G*	Exp.	RHF/3-21G	RHF/6-31G*
	1 (A)			**1 (IA)**		
Gd-O1	2.365 (.004)	2.334 (.035)	2.366 (.030)	-	2.341 (.034)	2.365 (.030)
Gd-N	2.655 (.006)	2.751 (.021)	2.824 (.020)	-	2.772 (.018)	2.868 (.018)
Gd-Ow	2.456	2.515	2.573	-	2.508	2.570
Gd-Pn[a]	1.633	1.744	1.839	-	1.792	1.927
Gd-Po[b]	0.719	0.625	0.555	-	0.637	0.600
ϕ[c]	36.0 (5.8)	39.0 (1.4)	37.2 (1.0)	-	-28.2 (1.2)	-24.2 (.9)
	2 (A)			**2 (IA)**		
Gd-O1	-	2.331 (.034)	-	-	2.334 (.033)	-
Gd-N	-	2.766 (.022)	-	-	2.782 (.019)	-
Gd-Ow	-	2.518	-	-	2.516	-
Gd-Pn	-	1.734	-	-	1.778	-
Gd-Po	-	0.640	-	-	0.651	-
ϕ	-	38.5 (1.3)	-	-	-27.9 (1.3)	-
	3 (A)			**3 (IA)**		
Gd-O1	2.350 (.007)	2.303 (.025)	2.323 (.020)	-	2.309 (.018)	-
Gd-N	2.617 (.028)	2.680 (.041)	2.755 (.063)	-	2.699 (.065)	-
Gd-N*[d]	2.566	2.677	2.757	-	2.654	-
Gd-Ow	2.466 (.049)[e]	2.545 (.002)	2.612 (.010)	-	2.554 (.015)	-
Gd-Pn	1.564	1.650	1.757	-	1.685	-
Gd-Po	0.749	0.767	0.694	-	0.775	-
ϕ	38.7 (3.3)	37.1 (4.4)	35.7 (4.2)	-	-27.4 (4.7)	-
	4 (A)			**4 (IA)**		
Gd-O1	2.361 (.029)	2.303 (.023)	2.319 (.020)	2.342 (.032)	2.304 (.016)	-
Gd-N	2.684 (.029)	2.689 (.038)	2.762 (.062)	2.652 (.031)	2.727 (.080)	-
Gd-N*[d]	2.574	2.670	2.739	2.585	2.628	-
Gd-Ow	2.494 (.046)	2.549 (.002)	2.620 (.006)	2.524 (.110)[e]	2.560 (.016)	-
Gd-Pn	1.630	1.637	1.737	1.606	1.685	-
Gd-Po	0.694	0.779	0.710	0.805	0.789	-
ϕ	38.2 (2.4)	37.0 (3.9)	35.5 (4.1)	-27.4 (2.4)	-26.5 (6.1)	-
	5					
Gd-O	2.389 (.019)	2.369 (.057)	2.413 (.050)			
Gd-N	2.666 (.056)	2.788 (.060)	2.821 (.046)			
Gd-Ow	2.463[e]	2.614	2.684			
Gd-P_{ax1}[f]	1.517	1.304	1.333			
Gd-P_{ax2}[g]	1.807	1.848	1.894			
Gd-P_{eq}[h]	0.109	0.345	0.345			
τ[i]	69.0 (4.0)	67.7 (8.0)	67.7 (7.9)			
$\theta_{ax1\text{-}eq}$[j]	6.7	11.8	12.3			
$\theta_{ax2\text{-}eq}$[k]	6.0	13.4	12.4			
	RHF/3-21G	RHF/6-31G*	DFT/6-31G*	RHF/3-21G	RHF/6-31G*	DFT/6-31G*
	1a (A)			**1a (IA)**		
Gd-O1	2.303	2.336	2.353	2.305	2.336	2.352
Gd-N	2.698	2.77	2.764	2.705	2.798	2.795
Gd-Pn	1.644	1.762	1.732	1.697	1.828	1.800
Gd-Po	0.728	0.651	0.741	0.751	0.709	0.794
ϕ	39.1	37.3	38.4	-28.2	-24.4	-25.4

[a] Distance of Gd from the least-squares plane defined by the N atoms, Pn. [b] Distance of Gd from the least-squares plane defined by the O atoms, Po. [c] Staggering of the P_O and P_N planes. [d] Nitrogen without acetate arm. [e] Distance between Gd and the acetate oxygen of the adjacent complex in the crystallographic cell. [f] Distance of Gd from the plane P_{ax1} defined by O2, O5, and O10. [g] Distance of Gd from the plane P_{ax2} defined by N2, O6, and O9. [h] Distance of Gd from the plane P_{eq} defined by N1, N3, and Ow. [i] Staggering between P_{eq} and the axial planes. [j] Tilt angle between P_{ax1} and P_{eq}. [k] Tilt angle between P_{ax2} and P_{eq}.

carboxylic oxygen atoms from the adjacent complex in the crystallographic cell.

In any case, the RHF/6-31G* geometries are closest to the experimental structures of the complexes. The greatest increment to the rms values comes from the position of the noncoordinated acetate oxygens: the conformational flexibility of acetates and their exposure on the molecular surface make these groups more susceptible to intermolecular interactions, causing distortion with respect to in vacuo results.

In all the calculated structures, the oxygen position of the capping water molecule is close to the experimental one. In the case of compound **1**, for which hydrogen positions are experimentally available,[44] it can be observed that the water hydrogen positions differ: in the crystallographic structure, the water is perpendicular to the acetate oxygen plane, while in the calculated one it is nearly parallel to the oxygen plane and involved in hydrogen bonds with the acetate oxygens.

In any case, the calculated Gd−N and Gd−Ow bond distances are greater, on average, than the corresponding experimental values; on the contrary, Gd−O bonds are shorter (3-21G) than or equal (6-31G*) to the experimental ones (Table 1). This suggests that the adopted ECP better describes bonds with higher ionic character.

Furthermore, the Gd−ligand (Gd−L) bonds calculated at the RHF/3-21G level are shorter than the corresponding RHF/6-31G* ones (Table 1). Indeed, as observed in the case of the $[Gd-(H_2O)_9]^{3+}$ system,[20] the 3-21G basis set is poor with respect to the Gd basis set; this unbalancing of basis sets induces the oxygen and nitrogen electrons to use the basis functions of the metal, thus providing the observed shortening in the Gd−L bonds. Comparison of the B-LYP/6-31G* and RHF/6-31G* results (compound **1a** in Table 1) shows that the inclusion of electron correlation causes only a negligible shortening of the Gd−L equilibrium values, whereas there is a significant

TABLE 2: Ab Initio Energies of the A Isomer (E_A, Hartree) and ab Initio and MM Relative Energies of the IA Isomer ($\Delta E = E_{IA} - E_A$, kcal mol^{-1}) for Compounds 1−4. For Compound 1, the Calculated Interconversion Barrier Values ($\Delta E^{\#} = E^{\#} - E_A$, kcal mol^{-1}) Are Also Reported[a]

compound	1			1a		2		3		4	
	E_A	ΔE	$\Delta E^{\#}$	E_A	ΔE	E_A	ΔE	E_A	ΔE	E_A	ΔE
experimental		0.8−1.4[b]	19 ± 2; 17 ± 1[c]								
ab initio											
RHF/3-21G//RHF/3-21G	−1540.13908	4.66	37.47	−1464.50233	3.72	−1695.42636	4.24	−1390.90231	4.53	−1507.36811	3.29
RHF/6-31G*// RHF/3-21G	−1548.42464	1.58	22.01	−1472.38710	0.89	−1704.55182	1.00	−1398.31803	0.90	−1515.41496	0.30
RHF/6-31G*// RHF/6-31G*	−1548.44145	1.68		−1472.40178	0.98						
DFT/6-31G*//RHF/3-21G	−1557.08643	3.01		−1480.66625	2.43						
DFT/6-31G*//RHF/6-31G*	−1557.07421	2.64		−1480.65510	1.93						
DFT/6-31G*//DFT/6-31G*				−1480.68597	1.95						
MM[d]											
set 1		1.48	52.95				4.32		4.46		0.18
set 2		1.45	47.24				4.50		4.68		0.00
set 1′		−4.62	21.52				−4.16		−3.58		−3.16
set 2′		−4.78	19.68				−4.34		−3.74		−3.44

[a] A concerted mechanism, involving the simultaneous rotation of all the acetate arms, was considered in the calculations. [b] Range calculated on the basis of the **A**/**IA** ratio for Eu and Tb complexes at 298 K.[39] [c] $\Delta H^{\#}$ values determined for the Yb[41] and Lu[47] complexes, respectively. [d] Parameters from RHF/3-21G PES (set 1) and RHF/6-31G* PES (set 2). The primed symbols highlight the exclusion of the electrostatic term from the force fields.

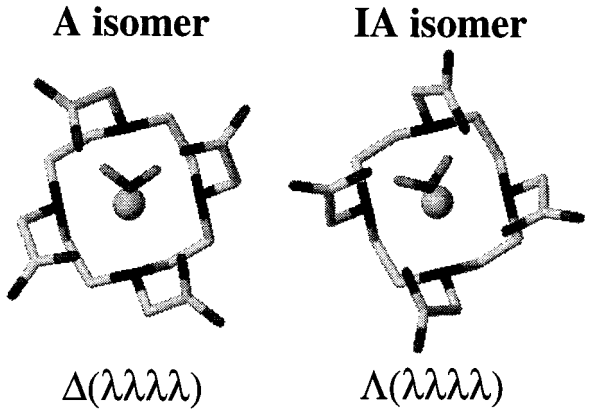

Figure 2. Conformational isomers of DOTA-like complexes: Δ and Λ refer to the helicity of the acetate arms, λ to that of the macrocycle.

shortening of the intraligand bond distances. These results are consistent with the ionic nature of the Gd−L bonds: electron correlation effects are relevant within the ligand fragment while the electrostatic nature of the metal−ligand interactions makes negligible the effects of electron correlation on the Gd−L bonds.

Conformational Energies. Ab initio calculations show that in compounds **1**−**4** the **A** isomer is always more stable than **IA** (Table 2). As previously discussed, experimental information on conformational equilibria in solution of these compounds cannot be achieved by NMR technique, due to the high magnetic moment of the Gd ion; the conformational behavior of Gd complexes can be inferred from data on other lanthanides. Thus, on the basis of ^{1}H NMR spectra analysis of lanthanide−DOTA complexes,[39,40] the **IA** isomer of compound **1** is expected 0.8−1.4 kcal mol^{-1} above **A**, and the interconversion barrier close to 17−19 kcal mol^{-1}.[41,47]

For compound **1**, the relative energy of the **IA** isomer calculated at both the RHF/6-31G*//RHF/3-21G and RHF/6-31G*//RHF/6-31G* levels is in close agreement with the expected experimental value (Table 2), whereas it is overestimated at the RHF/3-21G//RHF/3-21G level. The same trend is also observed for the calculated interconversion barrier of **1** (Table 2) and for the conformational energies of DOTA complexes with other lanthanides.[48] As far as the effects of the electron correlation are concerned, it can be seen (compounds **1** and **1a** in Table 2) that DFT/6-31G* relative energies are poorly affected by the level of geometry optimization and

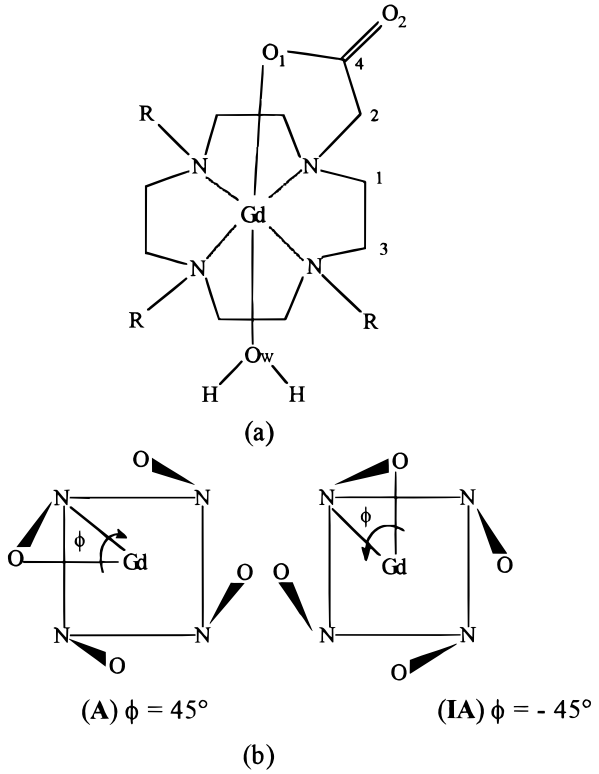

Figure 3. DOTA-like complexes **1**−**4**: (a) atomic numbering; (b) staggering (ϕ angle) between the nitrogen and oxygen planes in an ideal antiprismatic (**A**) and inverted antiprismatic (**IA**) arrangement.

substantially confirm the RHF stability scale, even if the ΔE values are slightly greater than those calculated at the RHF/6-31G* level. Thus, for these systems, where the ligand−ion interactions present a strong electrostatic character and, consequently, there is only a small charge transfer between ion and ligand, the correlation effects on the conformational energies can be considered negligible.

Summarizing ab initio results, we can conclude that geometry optimization can be confidently performed at the RHF/3-21G level; in fact, the computational effort required to use better ligand basis sets does not appear to be counterbalanced by significant improvement of the calculated geometries. Moreover, as RHF/6-31G* energies for compound **1** show the correct trend and are poorly affected by the geometry optimization level,

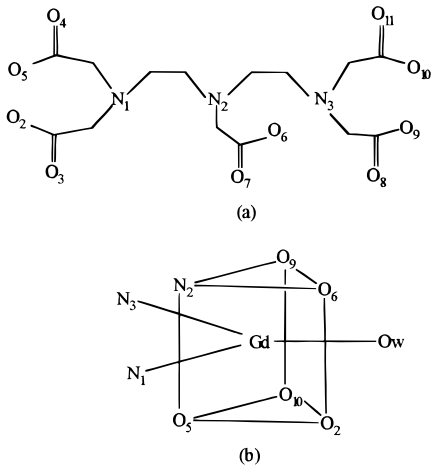

Figure 4. (a) atomic numbering and (b) coordination geometry around the ion in compound **5**.

TABLE 3: Average rms Values (Å) between the Experimental, ab Initio, and MM Structures of Compounds 1−5 (Both Isomers Are Considered When Data Are Available); rms Values Are Calculated on the Cartesian Coordinates of (I) Atoms of the Coordination Cages (Gd and the Ligand Coordinated Atoms); (II) Gd and All Ligand Atoms, but Hydrogens and Noncoordinated Acetate Oxygens; (III) All Complex Atoms, but Hydrogens

	RHF 3-21G	RHF 6-31G*	MM set 1	MM set 2	MM set 1′	MM set 2′
(I)						
exptl[a]	0.170	0.188	0.142	0.155	0.116	0.134
exptl[b]	0.239	0.228	0.209	0.224	0.161	0.172
RHF/3-21G			0.172	0.174	0.229	0.229
RHF/6-31G*			0.180	0.162	0.232	0.219
(II)						
exptl[a]	0.172	0.164	0.181	0.179	0.159	0.180
exptl[b]	0.211	0.193	0.203	0.205	0.171	0.189
RHF/3-21G			0.154	0.155	0.167	0.182
RHF/6-31G*			0.165	0.152	0.167	0.173
(III)						
exptl[a]	0.299	0.251	0.242	0.260	0.224	0.246
exptl[b]	0.320	0.267	0.259	0.278	0.228	0.249
RHF/3-21G			0.172	0.175	0.199	0.208
RHF/6-31G*			0.163	0.151	0.176	0.178

[a] rms values calculated omitting the water oxygen positions in the case of compounds **3**, **4** (**IA** isomer), and **5**. [b] rms values calculated by matching the calculated water positions with the corresponding experimental carboxylic oxygen positions in the case of compounds **3**, **4** (**IA** isomer), and **5**.

we assume that also for compounds **2**−**4**, where comparison with experiments is not feasible, a satisfactory representation of the PES is obtained by RHF/6-31G* energy calculations on RHF/3-21G optimized geometries.

III. Force Field Parameterization

Adopted Force Fields. Valence interactions involving Gd are handled in the framework of the point on a sphere (POS) approach.[23] In the POS scheme, the Gd−L stretching interactions are explicitly considered, while the L−Gd−L bending terms are replaced by the nonbonding interactions between the donor atoms (L···L); moreover, the torsional interactions involving the Gd−L bonds and the van der Waals interactions involving the metal are omitted. MM calculations were carried out using the Sybyl 6.2 molecular software package[49] using the TRIPOS force fields,[50] which is purely harmonic and without cross-terms. To deal with Gd−PAC complexes, three new types of interactions were added to the force fields: Gd−L stretching, Gd−L−X bending, and Gd−L−X−X torsional interactions (X denotes ligand atoms not coordinated to the metal). These interactions are treated with the standard potential functions of the TRIPOS force fields. Because MM calculations on Gd−PAC complexes have been performed either including or omitting the electrostatic term in the force fields, two different sets of parameters have been derived for the metal−ligand interactions.

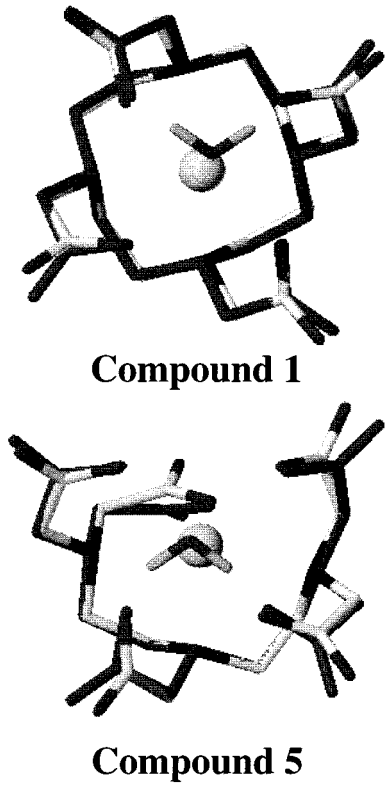

Figure 5. Superimpositions between the experimental (dark) and the RHF/3-21G (light) calculated structures of compounds **1** (**A** isomer) and **5**.

Metal-Independent Parameters. As in other applications of MM to coordination compounds,[22] force field parameters used for modeling the interactions in the free ligand have been assumed transferable to the ligand portion of the complex. The only exceptions are the C.3−C.3 and the C.3−C.2 stretching and the O.2−C.2−O.3 bending (list of the adopted atom types is reported in a note)[51]. In fact, it is well-known[22] that the L−X and X−X bonds are affected through delocalization of electron density to the metal upon coordination. The metal-independent parameters reported in Table 4 have been modified by a trial and error procedure to fit the ab initio calculated structures.

Metal-Dependent Parameters. The new parameters describing the stretching (Gd−N.4, Gd−O.3, and Gd−O.w) and the bending (Gd−N.4−C.3, Gd−O.3−C.2, and Gd−O.w−H.w) interactions were determined fitting the empirical potential to the ab initio PES of the $[Gd-DOTA(H_2O)]^{-1}$ complex as described later in this section. For the L−Gd−L−X torsions, the torsional constant values were set to zero; for the Gd−L−X−X torsions, the TRIPOS generalized parameters were used (Table 4). All the van der Waals interactions involving the Gd ion were omitted, setting to zero the value of the Gd nonbonding parameters. For the 1,3 nonbonding interactions between the L donor atoms, the standard van der Waals TRIPOS parameters were used, and when the electrostatic contribution is turned on, the electrostatic interactions between the L atoms were explicitly considered. For the electrostatic contribution calculation, the

TABLE 4: Force Field Parameters for the Gd−Ligand Interactions Determined by Fitting of the RHF/3-21G (Set 1 and Set 1′) and the RHF/6-31G* (Set 2 and Set 2′) PES of the A Isomer of Compound 1: the Primed Symbols Mean the Omission of the Electrostatic Contribution into the Force Field. For Metal-Independent Parameters, Default TRIPOS and Modified Values Are Reported[a]

	set 1	set 1′	set 2	set 2′
Metal-Dependent Parameters				
$r^0_{Gd-N.4}$	2.601	2.734	2.628	2.801
$K_{Gd-N.4}$	75.0	75.4	59.7	67.8
$r^0_{Gd-O.3}$	2.287	2.344	2.310	2.354
$K_{Gd-O.3}$	147.2	149.4	128.7	130.3
$r^0_{Gd-O.w}$	2.497	2.445	2.495	2.461
$K_{Gd-O.w}$	125.5	130.6	108.1	119.8
$\vartheta^0_{Gd-N.4-C.3}$	108.2	111.3	109.3	110.1
$K_{Gd-N.4-C.3}$	0.027	0.027	0.025	0.025
$\vartheta^0_{Gd-O.3-C.2}$	127.8	128.8	130.0	130.7
$K_{Gd-O.3-C.2}$	0.045	0.046	0.040	0.043
$\vartheta^0_{Gd-O.w-H.w}$	119.5	118.5	120.0	119.6
$K_{Gd-O.w-H.w}$	0.012	0.012	0.011	0.011
$K_{*-N.4-C.3-*}$[b]	0.27 (+3)		0.27 (+3)	
$K_{*-O.3-C.2-*}$[b]	4.50 (−2)		4.50 (−2)	

	default	modified
Metal-Independent Parameters		
$r^0_{C.3-C.3}$	1.540	1.510
$K_{C.3-C.3}$	633.6	650.0
$r^0_{C.3-C.2}$	1.501	1.530
$K_{C.3-C.2}$	639.0	639.0
$\vartheta^0_{O.3-C.2-O.2}$	120.0	126.0
$K_{O.3-C.2-O.2}$	0.030	0.030

[a] r^0 (Å); ϑ^0 (deg); K_r (kcal mol^{-1} Å^{-2}); K_ϑ (kcal mol^{-1} deg^{-2}); K_τ (kcal mol^{-1}). [b] Torsional force constant K_τ and torsional periodicity (in parentheses) are reported.

atomic charges fitted to the RHF/6-31G* molecular electrostatic potential (MEP) of the complexes[52] using the Merz−Kollman method[53] and a distance-dependent dielectric constant were used.

For the stretching and bending interactions the parametrization strategy developed by Maple and co-workers[13] was followed. Sampling of the ab initio PES was performed by moving the Gd ion inside the frozen coordination cage of the complex. This allows the mapping of the energy changes associated only with modifications of the internal coordinates involving the ion. In fact, the aim of parametrization is to determine the metal−ligand parameters, while the intraligand interactions are described by the predefined force fields.

Six new structures were generated starting from the RHF/3-21G optimized conformation of the **A** isomer of compound **1**. The relative energies of the sampled structures were within 20 kcal mol^{-1} above the minimum. The obtained distorted structures were checked to verify that the internal coordinates involving the metal were well sampled around equilibrium values: on average, a range of 0.4 Å for Gd−L bond distances and of 10° for Gd−L−X angles was obtained.

For each structure, the energy and the first derivatives with respect to the atomic Cartesian coordinates were calculated at the RHF/3-21G level. Only the first derivatives with respect to the Cartesian coordinates of the Gd atom and the nine L coordinated atoms were included in the fitting of the empirical potential. In fact, forces acting on these atoms strictly depend on the metal−ligand interactions, while those acting on the other atoms of the ligand mainly depend on the intraligand interactions. Finally, second derivatives of the energy were not considered due to the intrinsic limitations imposed by harmonic-diagonal force fields, like TRIPOS, on fitting information contained in the ab initio Hessian matrix.[13]

Thus, six relative energies and 210 first derivatives are available for the determination of 12 parameters. Parametrization was performed minimizing the object function **S**, defined as the weighted sum of the squared deviations between the ab initio and the MM quantities:

$$\mathbf{S} = w_E \sum_{k=1}^{N-1} [\Delta E_k^{\circ} - \Delta E_k(\mathbf{p})]^2 + w_g \sum_{k=1}^{N} \sum_{i=1}^{M} \sum_{j=1}^{3} \left[\frac{\partial E_k^{\circ}}{\partial x_{i,j}} - \frac{\partial E_k(\mathbf{p})}{\partial x_{i,j}} \right]^2$$

N is the number of sampled conformations, M is the number of atoms whose derivatives are considered; ΔE_k° and $\Delta E_k(\mathbf{p})$ are, respectively, the ab initio and the MM relative energies of the kth structure; $(\partial E_k^{\circ}/\partial x_{i,j})$ and $(\partial E_k(\mathbf{p})/\partial x_{i,j})$ are, respectively, the ab initio and the MM first derivatives with respect to the jth Cartesian coordinates of the ith atom of the kth structure. The values $w_E = 1$ and $w_g = 7 \times 10^{-4}$ (5×10^{-5} when the electrostatic contribution is turned off) are assigned to ensure that energy and first derivative squared deviations provide balanced contributions to the object function. The empirical potential parameters (**p** vector) are calculated, using a purposely developed computer code, by a least-squares procedure to fit the ab initio PES. Table 4 collects the force fields parameters obtained including (set 1) or omitting (set 1′) the electrostatic contribution.

To verify the influence of the ab initio PES calculation level on the force fields quality, the procedure was repeated, calculating relative energies and derivatives at the RHF/6-31G* level on six distorted structures generated from the RHF/6-31G* optimized geometry. The obtained parameter sets (set 2 and set 2′) are also reported in Table 4.

The quality of the PES fitting with the different sets of parameters is reported in Table 5: it can be noted that, independently of the inclusion of the electrostatic contribution, the empirical potentials are able to reproduce the respective ab initio PESs with the same accuracy. Comparison of the parameters (Table 4) shows that the RHF/3-21G derived sets present r^0 and ϑ^0 values smaller and force constant values greater than the corresponding RHF/6-31G* values, as a consequence of the steepest RHF/3-21G potential. Furthermore, when the electrostatic contribution is included, the force fields react with a shortening of the r^0 values to counterbalance the electrostatic repulsion among the donor atoms.

IV. Molecular Mechanics Calculations on Gd−PAC Complexes

To test the quality of the parameters derived from the ab initio PES of compound **1**, and their transferability to other Gd−PAC complexes, compounds **1**−**5** were optimized by MM using the different sets of parameters.

For compounds **1**−**4**, MM provides two minimum energy conformations (Table 2), corresponding to the previously discussed **A** and **IA** isomers, and for compound **5** one isomer presenting the correct tricapped trigonal prism arrangement around the metal (Table 6).

In general, MM calculations reproduce the experimental structures with the same accuracy of ab initio methods (Table 3), and, as previously observed for the ab initio results, the greatest increment to the rms values comes from the position of the noncoordinated acetate oxygens. Furthermore, the MM calculated Gd−N and Gd−O bond distances (Table 6) are,

TABLE 5: Fitting of the Empirical Potential to the RHF/3-21G (Set 1−1′) and RHF/6-31G* (Set 2−2′) PES: rms,[a] rrms,[b] and Maximum Deviations between ab Initio and MM Relative Energies (ΔE) and Gadolinium Gradient Norm ($||\mathbf{g}_{Gd}||$)

	ΔE			$||\mathbf{g}_{Gd}||$		
	rms (kcal mol^{-1})	rrms (%)	max. dev. (kcal mol^{-1})	rms (kcal mol^{-1} Å^{-1})	rrms (%)	max. dev. (kcal mol^{-1} Å^{-1})
set 1	0.78	8.7	1.82	11.1	14.7	17.6
set 1′	0.57	6.3	0.96	9.9	12.8	19.2
set 2	0.78	10.8	1.52	9.9	15.9	18.3
set 2′	0.85	11.7	1.52	10.5	16.9	15.5

[a] rms $= [\sum_k (X_k^o - X_k(\mathbf{p}))^2/N]^{1/2}$: N are the sampled conformations, X^o and $X(\mathbf{p})$ are the ab initio and MM calculated quantities. [b] rrms $= [\sum_k (X_k^o - X_k(\mathbf{p}))^2/\sum_k (X_k^o)^2]^{1/2}$.

TABLE 6: Values of the Main Geometrical Parameters (Refer to Table 1 for Their Definitions) of the MM Calculated Structures of Compounds 1−5. The Average Values Are Reported with Standard Deviations in Parentheses. Distances (Å), Angles (deg)

	expt	set 1	set 1′	set 2	set 2′
			1 (A)		
Gd−O1	2.365 (0.004)	2.357(0.017)	2.339(0.001)	2.381(0.020)	2.344(0.001)
Gd−N	2.655 (0.006)	2.756(0.019)	2.713(0.001)	2.804(0.022)	2.773(0.001)
Gd−Ow	2.456	2.495	2.451	2.489	2.461
Gd−Pn	1.633	1.702	1.594	1.772	1.665
Gd−Po	0.719	0.512	0.705	0.448	0.639
ϕ	36.0 (5.8)	41.7 (1.4)	38.7 (0.1)	40.8 (1.3)	38.1 (0.1)
			2 (A)		
Gd−O1		2.370 (0.014)	2.333 (0.001)	2.392 (0.017)	2.337 (0.001)
Gd−N		2.754 (0.022)	2.720 (0.001)	2.798 (0.025)	2.778 (0.000)
Gd−Ow		2.490	2.456	2.483	2.464
Gd−Pn		1.649	1.570	1.713	1.639
Gd−Po		0.530	0.744	0.466	0.676
ϕ		41.3 (1.3)	38.5 (0.1)	40.6 (1.2)	38.1 (0.1)
			3 (A)		
Gd−O1	2.350 (0.007)	2.338 (0.014)	2.343 (0.003)	2.358 (0.017)	2.348 (0.006)
Gd−N	2.617 (0.028)	2.701 (0.009)	2.722 (0.018)	2.744 (0.009)	2.784 (0.026)
Gd−N*	2.566	2.790	2.707	2.829	2.757
Gd−Ow	2.466 (0.049)[a]	2.490 (0.009)	2.454 (0.009)	2.479 (0.001)	2.464 (0.007)
Gd−Pn	1.564	1.670	1.632	1.740	1.702
Gd−Po	0.749	0.627	0.697	0.574	0.652
ϕ	38.7 (3.3)	41.0 (4.1)	38.4 (1.4)	40.0 (4.3)	37.3 (1.9)
			4 (A)		
Gd−O1	2.361 (0.029)	2.350 (0.011)	2.336 (0.005)	2.368 (0.013)	2.341 (0.007)
Gd−N	2.684 (0.029)	2.715(0.010)	2.729 (0.015)	2.754 (0.013)	2.793 (0.025)
Gd−N*	2.574	2.772	2.702	2.806	2.746
Gd−Ow	2.494 (0.046)	2.497 (0.009)	2.457 (0.010)	2.485 (0.004)	2.467 (0.007)
Gd−Pn	1.630	1.643	1.612	1.701	1.682
Gd−Po	0.694	0.711	0.711	0.664	0.661
ϕ	38.2 (2.4)	40.6 (2.8)	38.7 (1.2)	39.8 (3.0)	37.6 (1.7)
			5		
Gd−O	2.389 (0.019)	2.372 (0.016)	2.346 (0.009)	2.397 (0.016)	2.353 (0.010)
Gd−N	2.666 (0.056)	2.747 (0.036)	2.737 (0.017)	2.794 (0.042)	2.802 (0.019)
Gd−Ow	2.463[a]	2.517	2.452	2.507	2.460
Gd−P_{ax1}	1.517	1.275	1.335	1.261	1.299
Gd−P_{ax2}	1.807	1.852	1.858	1.879	1.871
Gd−P_{eq}	0.109	0.287	0.086	0.329	0.067
τ	69.0 (4.0)	67.6 (9.3)	68.8 (5.1)	67.4 (10.3)	68.6 (6.0)
θ_{ax1-eq}	6.7	18.0	13.9	17.7	13.2
θ_{ax2-eq}	6.0	13.0	5.1	12.5	4.4

[a] Distance between Gd and the acetate oxygen of the adjacent complex in the crystallographic cell.

respectively, greater than and equal to the corresponding experimental values, reflecting the characteristics of the ab initio PES from which the empirical potentials are derived. The quality of fitting between the MM and ab initio structures (Table 3) further highlights the agreement between MM and ab initio PESs.

In MM optimized structures, the oxygen positions of the water molecules are close to the experimental ones. The water molecules assume different orientations depending on the adopted force fields: when the electrostatic contribution is omitted, the water hydrogens point toward the external part of the complex, as experimentally observed; otherwise, when the electrostatic term is included, they are oriented toward the acetate oxygens atoms as in ab initio structures, because of hydrogen bond interactions.

The relative energies of the **IA** isomer calculated with the different sets of MM parameters for compounds **1**−**4** are reported in Table 2 together with the interconversion barrier values calculated for compound **1**. As previously discussed, the implemented sets of metal−ligand parameters are those that

best reproduce the ab initio potential around the ion, and not the whole PES of the complex, because the intraligand interactions are described by means of predefined force fields. Thus, MM conformational energies are not expected to reproduce the ab initio relative energies. Our results (Table 2) show that the ab initio stability scale can be qualitatively reproduced only including the electrostatic contribution, this contribution taking into account significant long-range components of the intraligand interactions.

V. Conclusions

Investigation of Gd−PAC complexes used as MRI contrast agents has shown that ab initio methods with the ECP approximation and properly parametrized MM method are powerful tools for modeling the conformational properties of these systems.

Due to the electrostatic nature of the metal−ligand interaction, the quality of ab initio geometries and relative energies is poorly affected by electron correlation, so calculations can be confidently performed at the RHF level. Furthermore, the use of the 3-21G basis set for the ligand is a good compromise between accuracy and computational effort, but reliable conformational energies can be calculated only at the RHF/6-31G* level.

The TRIPOS force field has been implemented with the parameters describing the interactions between Gd and PAC ligands. This new force field has been shown to be able to capture the main feature of the ab initio PES around the ion; furthermore the new parameters, used within the POS approach, provide a good description of the coordination cage around the ion and the complex conformations. Thus, the adopted procedure can be extended to the parametrization of interactions of lanthanides with ligands different from PAC when experimental data are not available.

In this procedure only the metal−ligand parameters are determined, while the intraligand interactions are described by means of a predefined force fields. Thus, because the MM conformational energies depend on both these interactions, also the parametrization of the intraligand interactions is needed to reproduce the whole ab initio PES of the complexes.

Finally, it has been shown that the electrostatic term is required to properly take into account intraligand long-range interactions and to obtain the right conformational energy trend. Moreover, the explicit inclusion of the electrostatic contribution into the empirical potential appears necessary for an adequate modeling of the interactions of these complexes with the solvent, these interactions playing a crucial role in the application of these systems as MRI contrast agents.

Acknowledgment. Computational support from CINECA and CILEA computational centers together with financial support from the Italian National Research Council (Grants CNR CT92.00040.12 and 94.04391.ST74) and the Italian Ministry of Scientific and Technological Research (Grants MURST 40% and 60%) are gratefully acknowledged.

Supporting Information Available: Values of the geometrical parameters of experimental and ab initio calculated structures of compounds **1** and **1a** (Table 1S and 2S); rms values between experimental and calculated (ab initio and MM) structures of compounds **1**−**5** (Table 3S and 4S); atomic charges of compounds **1**−**5** used in MM calculations (Table 5S) (5 pages). Ordering information is given on any current masthead page.

References and Notes

(1) Lauffer, R. B. *Magn. Reson. Q.* **1990,** *6*, 65.

(2) Tweedle, M. F. In *Lanthanide Probes in Life, Chemical and Earth Sciences*; Bünzli, J. C. G., Choppin, G. R., Eds.; Elsevier: Amsterdam, 1989.

(3) Lauffer, R. B. *Chem. Rev.* **1987**, *87*, 901.

(4) Rocklage, S. M.; Worah, D.; Kim, S. H. *Magn. Res. Med.* **1991**, *22*, 216.

(5) Cacheris, W. P.; Quay, S. C.; Rocklage, S. M. *Magn. Res. Imag.* **1990**, *8*, 467.

(6) Abbreviated names for the ligands are DOTA = 1,4,7,10-tetraazacyclododecane-1,4,7,10-tetraacetate; DOTMA = (1*R*,4*R*,7*R*,10*R*)-α′,α″,α‴,α⁗-tetramethyl-1,4,7,10-tetraazacyclododecane-1,4,7,10-tetraacetate; DO3A = 1,4,7,10-tetraazacyclododecane-1,4,7-triacetate; DO3MA = (1*R*,4*R*,7*R*)-α′,α″,α‴-trimethyl-1,4,7,10-tetraazacyclododecane-1,4,7-triacetate; DTPA = 1,4,7-triazaheptane-1,1,4,7,7-pentaacetate.

(7) Christiansen, P. A.; Ermler, W. C.; Pitzer, K. S. *Annu. Rev. Phys. Chem.* **1985**, *36*, 407.

(8) Krauss, M.; Stevens, W. J. *Annu. Rev. Phys. Chem.* **1984**, *35*, 357.

(9) Dolg, M.; Stoll, H.; Preuss, H. *J. Chem. Phys.* **1989**, *90*, 1730.

(10) Cundari, T. R.; Stevens, W. J. *J. Chem. Phys.* **1993**, *98*, 5555.

(11) Ross, R. B.; Gayen, S.; Ermler, W. C. *J. Chem. Phys.* **1994**, *100*, 8145.

(12) Dolg, M.; Stoll, H.; Savin, A.; Preuss, H. *Theor. Chim. Acta* **1989**, *75*, 173.

(13) Dolg, M.; Stoll, H. *Theor. Chim. Acta* **1989**, *75*, 369.

(14) Dolg, M.; Stoll, H.; Preuss, H. *Chem. Phys. Lett.* **1990**, *174*, 208.

(15) Dolg, M.; Stoll, H.; Flad, H. J.; Preuss, H. *J. Chem. Phys.* **1992**, *97*, 1162.

(16) Dolg, M.; Stoll, H.; Preuss, H. *Theor. Chim. Acta* **1993**, *85*, 441.

(17) Dolg, M.; Stoll, H.; Preuss, H. *J. Mol. Struct.* (*THEOCHEM*) **1991**, *235*, 67.

(18) Adamo, C.; Maldivi, P. *Chem. Phys. Lett.* **1997**, *268*, 61.

(19) Kaupp, M.; Schleyer, P. v. R.; Dolg, M.; Stoll, H. *J. Am. Chem. Soc.* **1992**, *114*, 8202.

(20) Cosentino, U.; Moro, G.; Pitea, D.; Calabi, L.; Maiocchi, A. *J. Mol. Struct.* (*THEOCHEM*) **1997**, *392*, 75.

(21) Landis, C. R.; Root, D. M.; Cleveland, T. *Molecular Mechanics Force Fields for Modeling Inorganic and Organometallic Compounds*, in Reviews in Computational Chemistry; Lipkowitz, K. B., Boyd, D. B., Eds.; VCH Publishers Inc.: New York, 1995; Vol. 6.

(22) Comba, P.; Hambley, T. W. *Molecular Modelling of Inorganic Compounds*; VCH Publishers Inc.: New York, 1995.

(23) Hay, B. P. *Coord. Chem. Rev.* **1993**, *126*, 177.

(24) Hay, B. P. *Inorg. Chem.* **1991**, *30*, 2876.

(25) Cundari, T. R.; Moody, E. W.; Sommerer, S. O. *Inorg. Chem.* **1995**, *34*, 5989.

(26) Beech, J.; Drew, M. G. B.; Leeson, P. B. *Struct. Chem.* **1996**, *7*, 153.

(27) Fossheim, R.; Dahl, S. G. *Acta Chem. Scand.* **1990**, *44*, 698.

(28) Maple, J. R.; Hwang, M. J.; Stockfish, T. P.; Dinur, U.; Waldman, M.; Ewig, C. S.; Hagler, A. T. *J. Comput. Chem.* **1994**, *15*, 162.

(29) Hwang, M. J.; Stockfish, T. P.; Hagler, A. T. *J. Am. Chem. Soc.* **1994**, *116,* 2515.

(30) Sun, H.; Mumby, S. J.; Maple, J. R.; Hagler, A. T. *J. Am. Chem. Soc.* **1994**, *116,* 2978.

(31) (a) Hill, J. R.; Sauer, J. *J. Phys. Chem.* **1994**, *98*, 1238. (b) Hill, J. R.; Sauer, J. *J. Phys. Chem.* **1995**, *99*, 9536.

(32) Frisch, M. J.; Trucks, G. W.; Schlegel, H. B.; Gill, P. M. W.; Johnson, B. G.; Robb, M. A.; Cheeseman, J. R.; Keith, T.; Petersson, G. A.; Montgomery, J. A.; Raghavachari, K.; Al-Laham, M. A.; Zakrzewski, V. G.; Ortiz, J. V.; Foresman, J. B.; Peng, C. Y.; Ayala, P. Y.; Chen, W.; Wong, M. W.; Andres, J. L.; Replogle, E. S.; Gomperts, R.; Martin, R. L.; Fox, D. J.; Binkley, J. S.; Defrees, D. J.; Baker, J.; Stewart, J. P.; Head-Gordon, M.; Gonzalez, C.; Pople, J. A. *Gaussian94*, Revision B.3; Gaussian, Inc.: Pittsburgh, PA, 1995.

(33) Calculations were performed on different computational platforms: Cray C90, Convex 3820, IBM RISC/6000 model 7030-3CT. As an example of the required CPU times, data relative to compound **1** are reported: one direct SCF plus gradient calculations, involving 345 (3-21G) or 490 (6-31G*) basis functions, required 1 h (3-21G) or 4 h (6-31G*) on Cray C90. Full geometry optimizations, involving 162 degrees of freedom, required 50 wave function evaluations (3-21G) to converge the gradient threshold (2 CPU days on Cray C90).

(34) (a) Becke, A. D. *Phys. Rev. A* **1988**, *38*, 3098. (b) Lee, C.; Yang, W.; Parr, R. G. *Phys. Rev. B* **1988**, *37*, 785.

(35) Dale, J. *Isr. J. Chem.* **1980**, *20*, 3.

(36) (a) Corey, E. J.; Bailar, J. C., Jr. *J. Am. Chem. Soc.* **1959**, *81*, 2620. (b) Beattie, J. K. *Acc. Chem. Res.* **1971**, *4*, 253.

(37) Kang, S. I.; Ranganathan, R. S.; Emswiller, J. E.; Kumar, K.; Gougoutas, J. Z.; Tweedle, M. F. *Inorg. Chem.* **1993**, *32*, 2912.
(38) Kumar, K.; Chang, C. A.; Francesconi, L. C.; Dischino, D. D.; Malley, M. F.; Gougoutas, J. Z.; Tweedle, M. F. *Inorg. Chem.* **1994**, *33*, 3567.
(39) Hoeft, S.; Roth; K. *Chem. Ber.* **1993**, *126*, 869.
(40) Aime, S.; Botta, M.; Fasano, M.; Marques, M. P. M.; Geraldes, C. F. G. C.; Pubanz, D.; Merbach, A. E. *Inorg. Chem.* **1997**, *36*, 2059.
(41) Jacques, V.; Desreux, J. F. *Inorg. Chem.* **1994**, *33*, 4048.
(42) Brittain, G. H.; Desreux, J. F. *Inorg. Chem.* **1984**, *23*, 4459.
(43) Dubost, J. P.; Legar, J. M.; Langlois, M. H.; Meyer D.; Schaefer, M. *C. R. Acad. Sci. Paris, Ser. 2* **1991**, *312*, 349.
(44) Chang, C. A.; Francesconi, L. C.; Malley, M. F.; Kumar, K.; Gougoutas, J. Z.; Tweedle, M. F.; Lee, D. W.; Wilson, L. J. *Inorg. Chem.* **1993**, *32*, 3501.
(45) Inoue, M. B.; Inoue, M.; Fernando, Q. *Inorg. Chim. Acta* **1995**, *232*, 203.
(46) Jenkins, B. J.; Lauffer, R. B. *Inorg. Chem.* **1988**, *27*, 4730.
(47) Aime, S.; Barge, A.; Botta, M.; Fasano, M.; Ayala, J. D.; Bombieri, G. *Inorg. Chim. Acta* **1996**, *246*, 423.
(48) Cosentino, U.; Moro, G.; Pitea, D.; Villa, A.; Maiocchi, A. To be published.
(49) *SYBYL 6.2*; Tripos Associates: 1699 S. Hanley Road, Suite 303, St. Louis, MO 63144, 1992.
(50) Clark, M.; Cramer, R. D., III; Van Opdenbosch, N. *J. Comput. Chem.* **1989**, *10*, 982.
(51) List of the TRIPOS force field atom types used in the definition of the Gd−PAC complexes: Gd (gadolinium); C.3 (sp^3 carbon); C.2 (sp^2 carbon); N.4 (tetracoordinated sp^3 nitrogen); O.3 (sp^3 oxygen); O.2 (sp^2 oxygen); O.w (sp^3 water oxygen); H (hydrogen); H.w (water hydrogen). In all cases, TRIPOS default atomic parameter values are used. The O.w and H.w atom types have been included only for the purpose of distinguishing the water O and H from the ligand O and H: the atomic parameters for O.w and H.w have been set equal to those of O.3 and H, respectively.
(52) As the potential derived charges of atoms with the same MM type presented close values, their average value was considered in MM calculations. Nitrogen atom charges in compounds **3** and **4** were averaged only for those nitrogens that carry the acetate arms.
(53) Besler, B. H.; Merz, K. M.; Kollman, P. A. *J. Comput. Chem.* **1990**, *11*, 431.